

# A Precision Environment-Wide Association Study of Hypertension via Supervised Cadre Models

Alexander New<sup>1,2</sup>

NEWA@RPI.EDU

Kristin P. Bennett<sup>1,2</sup>

BENNEK@RPI.EDU

<sup>1</sup>*Institute for Data Exploration and Applications*

<sup>2</sup>*Department of Mathematical Sciences*

*Rensselaer Polytechnic Institute*

*Troy, NY, USA*

## Abstract

We consider the problem in precision health of grouping people into subpopulations based on their degree of vulnerability to a risk factor. These subpopulations cannot be discovered with traditional clustering techniques because their quality is evaluated with a supervised metric: the ease of modeling a response variable over observations within them. Instead, we apply the supervised cadre model (SCM), which does use this metric. We extend the SCM formalism so that it may be applied to multivariate regression and binary classification problems. We also develop a way to use conditional entropy to assess the confidence in the process by which a subject is assigned their cadre. Using the SCM, we generalize the environment-wide association study (EWAS) workflow to be able to model heterogeneity in population risk. In our EWAS, we consider more than two hundred environmental exposure factors and find their association with diastolic blood pressure, systolic blood pressure, and hypertension. This requires adapting the SCM to be applicable to data generated by a complex survey design. After correcting for false positives, we found 25 exposure variables that had a significant association with at least one of our response variables. Eight of these were significant for a discovered subpopulation but not for the overall population. Some of these associations have been identified by previous researchers, while others appear to be novel associations. We examine several learned subpopulations in detail, and we find that they are interpretable and that they suggest further research questions.

## 1. Introduction

Precision health approaches (Colijn et al. (2017)) are increasingly being adopted in health analytics. In them, people with different characteristics are modeled as having different levels of vulnerability and resistance to a harmful condition. For example, Gathirua-Mwangi et al. (2015) found that, for non-Hispanic Black women, there was a significant association between developing breast cancer and becoming overweight; however, this significant association did not appear in other cohorts of women. Thus, making proper use of properly chosen subpopulations is important when analyzing complex health problems. When possible, as in the above example, domain knowledge should be used to infer what subpopulations are useful for a given precision health problem. In cases where the existing knowledge is not sufficiently complete to do this, machine learning methods can discover informative subpopulations that lie latent in large heterogenous datasets.

In this work, we develop a novel machine learning method for health risk analysis problems. This method is based on the supervised cadre model (SCM), proposed in New et al. (2018). The SCM discovers subpopulations and assigns each subpopulation a simple model. Sparsity-inducing regularization (Tibshirani (1994)) ensures that subpopulations are defined via simple rules – for example, subjects above a certain threshold based on age and BMI vs. those below it. This means that subpopulations suggested by an SCM are easily validated by a domain expert, granting them a useful form of interpretability (Lipton (2016)).

We can use the SCM for any type of risk analysis problem, but, here, we focus on two cases. In the first, the response is the vector of a subject’s diastolic and systolic blood pressure readings (DBP and SBP), which we jointly refer to as continuous blood pressure (CBP). Here the risk analysis is based on multivariate regression. In the second, the response is whether or not a subject’s blood pressure is high enough to classify them as having hypertension (HYP), so binary classification is used.

The SCM has two primary components. The first is the cadre membership function, which assigns every subject a distribution characterizing that subject’s probability of belonging to each cadre. The second component of an SCM is a set of score-prediction models, one for each cadre. These predict the expected response score of that subject, supposing they were known to belong to a specific cadre. For HYP, the score-prediction models output a scalar risk score. For CBP, the score-prediction functions output a two-dimensional vector containing the predicted systolic and diastolic blood pressures. Thus, the same cadre structure is used for both SBP and DBP predictions, although each may have different regression weights.

Importantly, the cadre membership function and score-prediction functions are learned simultaneously. Rather than being chosen to minimize an unsupervised quantity such as within-cluster-sum-of-squares, cadres are selected to maximize the effectiveness of the score-prediction process. Only a small subset of covariates are used for the the cadre-assignment and target-prediction processes – their functions are sparse with respect to subject characteristics (Tibshirani (1994)). The cadre membership function and each cadre’s target-prediction function are allowed to use a different set of covariates.

We use the SCM to carry out an environment-wide association study (EWAS, Patel et al. (2010)). This class of study analyzes the association between one or more response condition(s) – for us, blood pressure and hypertension – and many different environmental exposure risk factors, such as trace metals and pesticides. Using the supervised cadre method, we generalize existing environmental exposure risk analysis methods. These methods often consider only a small number of possible risk factors, and they are typically restricted to either population-level analysis, or to analysis over a small set of explicitly-chosen subpopulations.

Smaller association studies have been carried out for blood pressure and hypertension (e.g., Trasande et al. (2013), Shiue (2014), Gallagher and Meliker (2010)). Some of these have used our dataset, the National Health and Nutrition Examination Survey (NHANES, Centers for Disease Control and Prevention (CDC)), a publicly accessible, cross-sectional examination of the American population. However, a large-scale hypertension EWAS has not yet been performed.

The SCM discovers twenty-five risk factors that have a significant association with DBP, SBP, or HYP. Of these, eight are identified as significant risk factors because we used

subpopulation-based modeling. Some of these risk factors have been identified in previous studies, and others have not. We analyze the subpopulations discovered by the SCM, and we demonstrate how they may be presented to a domain expert for validation.

### 1.1 Related Works

The supervised cadre model learns a soft (i.e., probabilistic) partition of subject-space, and then each element of this partition is assigned an interpretable linear model. This can be viewed as a modification of a simple hierarchical mixture of experts (HME, Jordan and Jacobs (1994)). However, the SCM uses a different gating function than the HME does. Its parameterization lets the elements of the partition be interpreted as subpopulations centered around a mean-subject.

The SCM is comparable to semi-supervised clustering (e.g. Demiriz et al. (1999)), because both approaches deal with incomplete label information. In semi-supervised clustering, the training set is divided into a set of labeled and unlabeled observations, and supervised and unsupervised metrics are combined to learn a single model. Given a dataset corresponding to a  $K$ -label classification problem, the  $M$ -cadre SCM learns a model that assigns to an observation with class  $k$  a joint class-cadre label from the set  $\{(1, k), \dots, (M, k)\}$ . To improve interpretability, the SCM uses feature selection in its cadre-assignment procedure. Unsupervised methods have also used feature selection. Examples include the sparse  $k$ -means (Witten and Tibshirani (2010)) and weighted fuzzy  $c$ -means (Wang et al. (2004)) methods. These methods solve problems that lack a usable response variable, and sparse  $K$ -means focuses on those in the  $p \gg n$  regime. Our interest is supervised learning problems, as our goal is the discovery of subpopulations that provide useful information about the variation of a response variable.

When performing risk analysis with the SCM, we want discovered subpopulations to be easily validated by a health expert. This requires model interpretability. Lipton (2016) and Doshi-Velez and Kim (2017) have proposed different ways to characterize the degree to which a model is interpretable, such as simulability, decomposability, and amicability to post-hoc interpretation. The SCM is simulatable because a human can easily replicate a model's prediction. It is decomposable because all of its parameters have intuitive purposes. It also admits post-hoc interpretations because variable distributions can be grouped by subpopulation for visualization.

## 2. Methods

### 2.1 Supervised Cadre Models

In this section, we describe the mathematical formalism behind the learning and prediction processes for a supervised cadre model. New et al. (2018) only used the SCM for scalar regression problems. In this work, we extend the range of problems the SCM can be applied to. Let a subject be represented by  $x \in \mathbb{R}^P$  and let the response be  $y \in \mathcal{Y} \subseteq \mathbb{R}^{P_Y}$ . For hypertension,  $P_Y = 1$  and  $\mathcal{Y} = \{-1, +1\}$ ; for continuous blood pressure,  $P_Y = 2$  and  $\mathcal{Y} = \mathbb{R}^{P_Y}$ . In an EWAS, the measurements constituting a vector  $x$  contain a set of control variable values (e.g. age and ethnicity) and a single environmental risk factor. Control variables and general experiment design are discussed in detail in Section 3.1.

Let  $F_P = \{1, \dots, P\}$  be the full set of covariate indices. We choose index sets  $F_C, F_T \subseteq F_P$ , with  $P_C = |F_C|$  and  $P_T = |F_T|$ . If  $p \in F_C$ , then the covariate  $x_p$  is used to determine which cadre a subject  $x$  belongs to. If  $p \in F_T$ , then the covariate  $x_p$  is used to predict the response. In our analysis, we set  $F_C$  equal to the set of control variable indices. We set  $F_T$  equal to the union of  $F_C$  and the index corresponding to the single risk factor.

Let  $M$  be the number of cadres in the model. We define a score function  $f : \mathbb{R}^P \rightarrow \mathbb{R}^{P_Y}$  that may be factored as  $f(x) = g(x_{F_C})^T e(x_{F_T})$ , where  $g(x_{F_C}) = [g_1(x_{F_C}) \dots g_M(x_{F_C})] \in \mathbb{R}^M$  and  $e(x_{F_T}) = [e^1(x_{F_T}) \dots e^M(x_{F_T})] \in \mathbb{R}^{P_Y \times M}$ . Here,  $g_m(x_{F_C})$  is the probability that subject  $x$  belongs to cadre  $m$ , and  $e^m(x_{F_T}) \in \mathbb{R}^{P_Y}$  is the expected response value for  $x$  if  $x$  were known to be in cadre  $m$ .

The SCM imposes the following parametric forms on  $g$  and  $e$ :

$$g_m(x_{F_C}) = \frac{e^{-\gamma \|x_{F_C} - c^m\|_d^2}}{\sum_{m'} e^{-\gamma \|x_{F_C} - c^{m'}\|_d^2}} \quad \text{and} \quad e^m(x_{F_T}) = (W_m)^T x_{F_T} + w_0^m.$$

Here:  $\|z\|_d = \left( \sum_p |d_p| (z_p)^2 \right)^{1/2}$  is a seminorm;  $d$  is a feature-selection parameter used for cadre assignment; each  $c^m \in \mathbb{R}^{P_C}$  is the center of the  $m$ th cadre; each pair  $W_m \in \mathbb{R}^{P_T \times P_Y}, w_0^m \in \mathbb{R}^{P_Y}$  characterizes the regression hyperplane for cadre  $m$ ; and  $\gamma > 0$  is a hyperparameter that controls the sharpness of the cadre-assignment process. Thus, the cadre membership of  $x$  is a multinoulli random variable with probabilities  $\{g_1(x_{F_C}), \dots, g_M(x_{F_C})\}$ ; this set is the softmax (Murphy (2012)) of the set of weighted inverse-distances  $\{\gamma \|x_{F_C} - c^1\|_d^{-2}, \dots, \gamma \|x_{F_C} - c^M\|_d^{-2}\}$ .

If we let  $C = \{c^1, \dots, c^M\}$ ,  $W = \{W_1, \dots, W_M\}$ , and  $W_0 = \{w_0^1, \dots, w_0^M\}$ , the SCM is fully specified by the the parameters  $C, d, W, W_0$ , and the hyperparameter  $\gamma > 0$ . We group a model's parameters as  $\Theta = \{C, d, W, W_0\}$ . All the parameters have interpretations, ensuring model decomposability (Lipton (2016)). Each  $c^m$  is the center of the  $m$ th cadre. The coefficient  $d_p$  indicates how important the  $p$ th feature is for the cadre-assignment process. Each cadre has one or more regression hyperplanes characterized by  $W_m$  and  $w_0^m$ .

## 2.2 Learning an SCM

The training process for the SCM is similar for the HYP and CBP cases. In both cases, we first specify a probabilistic model  $p(y|x)$ , and then we use Bayesian point estimation to learn the model. We model CBP with

$$y|x \sim \mathcal{N}(f(x), \Sigma) \quad \Sigma = \begin{bmatrix} \sigma_{sbp}^2 & 0 \\ 0 & \sigma_{dbp}^2 \end{bmatrix} \in \mathbb{R}^{P_Y \times P_Y}.$$

For HYP, we adopt the probabilistic model  $p(y|x) \propto e^{-\max\{0, 1 - yf(x)\}}$ . Thus, modeling continuous blood pressure requires an additional parameter compared to hypertension:  $\Sigma$ . Let  $\Theta_{full} = \Theta$  if the response is hypertension, and let  $\Theta_{full} = \Theta \cup \{\Sigma\}$  if the response is continuous blood pressure. Let  $X = \{x^n\}_{n=1}^N$  be the set of training data, with associated response values  $Y = \{y_n\}_{n=1}^N$ . Then the optimal parameters  $\Theta_{full}$  are a solution to the log-posterior maximization problem

$$\max_{\Theta_{full}} \log p(\Theta_{full}|X, Y) = \log p(Y|X, \Theta_{full}) + \log p(\Theta_{full}).$$

Now we discuss the prior  $p(\Theta_{full})$ . When the response is blood pressure, we factor the prior as  $p(\Theta_{full}) = p(d|\Sigma)p(W|\Sigma)p(\Sigma)$ , and when the response is hypertension, the prior factors as  $p(\Theta_{full}) = p(d)p(W)$ . In both cases, we assign  $W$  and  $d$  elastic-net (Zou and Hastie (2005)) priors to encourage sparse but stable models. The covariance parameters are given uninformative priors (Gelman et al. (2013)):  $p(\sigma^2) \propto 1/\sigma^2$  for both  $\sigma_{sbp}$  and  $\sigma_{dbp}$ .

The SCM learning problem requires the specification of the following hyperparameters: the number of cadres  $M$ , the cadre-sharpness  $\gamma$ , the elastic-net mixing weights  $\alpha_d$  and  $\alpha_W$ , and the regularization strengths  $\lambda_d$  and  $\lambda_W$ . Once these are specified, we learn the model via stochastic gradient descent in Tensorflow (Abadi et al. (2015)); the specific solver is Adam (Kingma and Ba (2014)), which uses adaptive stepsizes for faster convergence. Thus, the final optimization problem for HYP is

$$\hat{\Theta}_{full} = \arg \max_{\Theta_{full}} \left\{ - \sum_{n=1}^N w_n \max\{0, 1 - y_n f(x^n)\} + \log p(d) + \log p(W) \right\}, \quad (1)$$

where  $\log p(d) = -\lambda_d(\alpha_d||d||_1 + (1-\alpha_d)||d||_2^2)$ ,  $\log p(W)$  is defined similarly, hyperparameters are omitted for brevity, and  $w_n$  is the survey weight for the  $n$ th subject. Section 2.3 describes the survey weights in greater detail. The final optimization problem for CBP is very similar. The SCM learning problem is nonconvex and non-differentiable, but New et al. (2018) report that, when trained using SGD, all discovered local minimizers tend to be of comparable quality. Thus, we do not worry about poor-quality minimizers in this work.

### 2.3 Risk Analysis on Survey Data

In this paper, we solve risk analysis problems that are formulated as binary classification and multivariate regression tasks. The goal is to use statistical modeling and significance tests to identify covariates that are strongly associated with the response in one or more of the subpopulations discovered with the SCM. We do not expect to learn models with low out-of-sample error, because hypertension is a complex phenomenon that is affected by lifestyle, dietary, environmental, and genetic factors (Trasande et al. (2013)). NHANES, however, has no genetic variables, and its lifestyle and dietary variables are based on questionnaires, which makes them more likely to be biased (Patel et al. (2010)).

Each wave of NHANES is constructed via a complex survey design (CSD, Heeringa et al. (2017)). In the NHANES CSD, the survey population is divided according to a multistage sample design based on counties and households, and certain minority subpopulations like the elderly are oversampled relative to their absolute size in the population. A given subject's role in the NHANES CSD is captured by their survey weight, survey stratum, and survey variance unit. More details about complex survey designs can be found in a standard reference such as Heeringa et al. (2017).

When analyzing data generated by a CSD, it is important to use appropriate modeling techniques. Specifically, observations in a CSD are not sampled *iid*, and the use of modeling techniques that assume *iid* will produce biased results. Incorporation of survey weights is necessary to attain correct parameter point estimates, and incorporation of strata and variance units is necessary for valid standard error estimates and confidence intervals. We incorporate survey weights into the SCM loss function (1) with the  $w_n$  terms. This means the SCM's parameter point estimates will be valid. Incorporation of survey strata and

variance units for valid standard error estimation requires the use of survey-weighted generalized linear models (GLMs), which are implemented in the `survey` package for R (Lumley (2016)). The process by which we switch from the SCM to survey-weighted analysis is described in Section 2.4.

## 2.4 Applying Conditional Entropy to Assess Cadre Hardness

In this section, we discuss how the soft partition learned by an SCM is combined with survey-weighted modeling. Given an SCM, we take every subject and assign them to their most likely cadre, “hardening” the soft, probabilistic cadre assignments.

We evaluate the validity of this simplification with a novel application of conditional entropy (Murphy (2012)). In order for the simplification to be valid, any given subject must be very confidently assigned to its most likely cadre. That is, for any subject  $x$ , we desire  $g_m(x) \approx 0$  or  $g_m(x) \approx 1$ . Conditional entropy describes the extent to which this condition holds; it measures how “hard” a probabilistic partition is.

Let  $X_m$  be the set of subjects  $x$  such that  $g_m(x) \geq g_{m'}(x)$  for  $m' \in \{1, \dots, M\}$ . Let  $C \in \{1, \dots, M\}$  be the random variable with conditional probability mass function  $p(C = m|x) = g_m(x) = p(\{x \in X_m\})$ , for any subject  $x$ . That is,  $C$  is the random variable of conditional cadre assignments. Then the conditional entropy

$$H(C|\{x \in X_m\}) = - \sum_{m'} p(C = m'|\{x \in X_m\}) \log_2 p(C = m'|\{x \in X_m\})$$

quantifies how confident the assignment of subjects into cadre  $X_m$  tends to be. If  $H(C|\{x \in X_m\})$  is close to 0, then cadre assignments are very confident. As  $H(C|\{x \in X_m\})$  approaches its maximum value of  $\log_2 M$ , cadre assignments become less confident, and our deterministic partition approximation becomes less valid.

## 3. Data and Variables

Our data source is the National Health and Nutrition Examination Survey (NHANES), a publicly accessible, cross-sectional examination of the American population. NHANES is administered every two years, and the results are released in units called waves. For our EWAS, we used the 1999 through 2013 waves.

NHANES divides its variables into components, from which we used demographic variables (for subject age, gender, ethnicity, and socioeconomic status), examination variables (for subject BMI), and laboratory variables (for environmental exposure variables). We draw potential risk factors from sixteen classes of environmental exposure variables, such as arsenics and polyaromatic hydrocarbons. The sixteen classes are subdivided further into 38 categories for reasons described in Section 3.1. The full list of categories is in Table 1.

### 3.1 Choosing Variables

We defined our response variables as follows. An NHANES participant has their blood pressure taken at least three times. We averaged all of a participant’s blood pressure readings and used the averaged systolic and diastolic blood pressure readings as a vector response; this procedure was also used by Trasande et al. (2013). We also defined a binary response

variable for the hypertension (HYP) condition by saying that a subject has hypertension if their average systolic BP is at least 140 mmHg and their average diastolic BP is at least 90 mmHg; this procedure was used in Shiue (2014).

When estimating the association of a potential risk factor with a response variable in risk analysis, it is common to control for known confounders. For blood pressure, we followed Shiue (2014) and controlled for age, sex, ethnicity, and body mass index. Some environmental exposure variables were measured in the subjects' urine. When analyzing those variables, we also controlled for urinary creatinine, as is frequently done in environmental risk factor studies (e.g., Shiue (2014) and Trasande et al. (2013)). We refer to these as the study's control variables.

We extract 218 environmental exposure potential risk factors for analysis, grouped into 38 categories. We need to define these categories because, in NHANES, a given environmental exposure variable will not, in general, be measured on an entire wave's participants, nor will it be measured in every wave. This gives the full NHANES dataset a block-sparse structure. To account for this structure, we divide the classes of risk factors into categories that have all been measured in the same subjects during the same waves. For example, the category PHT4 contains six phthalates that were measured on the same subset of the survey population in waves 2005 through 2013. Table 1 gives the number of subjects and risk factors in each category, as well as the waves in which it is present.

Category	Category Description	Waves	# RFs	$N_{tot}$	$N_{pos}$
ARS1	Arsenics	2003, 2005, 2007, 2009, 2011, 2013	6	12421	270
ARS2	Arsenics	2003, 2005, 2007, 2009, 2011	2	10277	225
CLM1	Metals, Blood	2003, 2005, 2007, 2009	3	25518	561
DEE1	DEET & Metabolites	2007, 2009, 2011, 2013	3	8029	187
DIO1	Dioxins, Furans, Coplanar PCBs	1999, 2001, 2003	7	5063	133
DIO2	Dioxins, Furans, Coplanar PCBs	1999, 2001, 2003	18	3777	117
DIO3	Dioxins, Furans, Coplanar PCBs	1999, 2001	13	3353	89
DIO4	Dioxins, Furans, Coplanar PCBs	1999, 2001	10	2068	68
DIO5	Dioxins, Furans, Coplanar PCBs	2001, 2003	3	2581	78
DIO6	Dioxins, Furans, Coplanar PCBs	1999, 2003	1	3170	87
EST1	Phytoestrogens	2003, 2005, 2007, 2009	6	8239	178
IMB1	Mercury, Blood	2005, 2007, 2009, 2011, 2013	1	28600	638
IMB2	Mercury, Blood	2011, 2013	2	9426	212
IMU1	Mercury, Urine	2003, 2005, 2007, 2009, 2011	1	10346	225
INS1	Organophosphate Insecticides	2003, 2005, 2007	6	5888	131
PAH1	Polyaromatic Hydrocarbons	2003, 2005, 2007, 2009, 2011, 2013	6	11831	255
PAH2	Polyaromatic Hydrocarbons	2003, 2005, 2007, 2009, 2011	2	9967	217
PCH1	Polyfluoralkyl Chemicals	2003, 2005, 2007, 2009, 2011, 2013	7	11068	275
PCH2	Polyfluoralkyl Chemicals	2003, 2005, 2007, 2009, 2011	4	9170	221
PCU1	Pesticides, Current-use	1999, 2001, 2003	4	5247	111
PCU2	Pesticides, Current-use	2003, 2005, 2007	17	4408	90
PCU3	Pesticides, Current-use	1999, 2001	16	3153	65
PEN1	Pesticides, Environmental	2003, 2005, 2007, 2009, 2011	2	10240	231
PEN2	Pesticides, Environmental	2003, 2005, 2007, 2009	3	8329	188
PHE1	Environmental Phenols & Parabens	2003, 2005, 2007, 2009, 2011	3	10234	231
PHE2	Environmental Phenols & Parabens	2005, 2007, 2009	5	6284	141
PHT1	Phthalates	2005, 2007, 2009, 2011, 2013	2	10315	238
PHT2	Phthalates	2003, 2005, 2007, 2009, 2011, 2013	1	12416	276
PHT3	Phthalates	1999, 2001, 2003, 2005, 2007, 2009, 2011, 2013	5	16518	373
PHT4	Phthalates	1999, 2001	6	3614	87
PHT5	Phthalates	2001, 2003, 2005, 2007, 2009, 2011, 2013	4	14609	332
PHT6	Phthalates	1999, 2001, 2003, 2005, 2007, 2009	2	12491	276
PHT7	Phthalates	2001, 2003, 2005, 2007, 2009, 2011	1	12489	278
UMT1	Metals, Urine	1999, 2001, 2003, 2005, 2007, 2009, 2011, 2013	9	15824	354
UMT2	Metals, Urine	2001, 2003, 2005, 2007, 2009, 2011, 2013	1	14571	312
UMT3	Metals, Urine	1999, 2001, 2003, 2005, 2007, 2009	2	12331	276
VOL1	Volatile Organic Compounds	2005, 2011, 2013	27	6072	141
VOL2	Volatile Organic Compounds	1999, 2001, 2005, 2013	7	5701	155

Table 1: Summary of datasets. # RFs is the number of risk factors in a category,  $N_{tot}$  is the total number of subjects in that category's dataset, and  $N_{pos}$  is the number of subjects with hypertension in that category's dataset.

## 4. Significance Results and Subpopulation Exploration

### 4.1 Study Design

We summarize our study design with Algorithms 1 and 2. The former describes the process by which our supervised cadre models were trained. We used grid search to choose the optimal  $\lambda_d$  and  $\lambda_W$ ; the metric for model-goodness was the Bayesian Information Criterion (BIC). When choosing the best SCM, we restricted our attention to models that had cadre-assignment conditional entropies  $H(C|x \in X_m)$  of no more than 0.20 for all  $m$ . This ensures that the deterministic approximation of the soft partition is not unrepresentative. To allow the conditional entropies to be small, we set the cadre-sharpness hyperparameter  $\gamma$  to 75. Because we want sparse cadre structures, we favor  $\ell^1$  regularization and set the elastic-net mixing hyperparameters  $\alpha_d$  and  $\alpha_W$  to 0.9. We learn SCMs with  $M = 1, 2, 3$  different cadres: forays into larger values of  $M$  yielded models with prohibitively high BIC scores, suggesting a saturation of the dataset with respect to model complexity. Note that the model selection and learning is done independently for every risk factor.

```

Input: Response-variable, control-variables, set of risk factor categories, number of
cadres  $M$ , grid of values for  $(\lambda_d, \lambda_W)$ , cadre-assignment sharpness  $\gamma$ , regularization
strengths  $\lambda_d, \lambda_W$ 
Output: Set of optimal models
for every category of risk factors in categories do
    Log transform environmental exposure variables
    Mean-center and standardize data, including response if modeling CBP
    for every risk-factor in category do
        for every  $\lambda_d, \lambda_W$  do
            Learn an SCM to predict response-variable using risk-factor and all
            control-variables with  $M, \lambda_d, \lambda_W, \alpha_d, \alpha_W, \gamma$  as hyperparameters
            Calculate  $H(C|x \in X_m)$  for  $m = 1, \dots, M$ 
        end
        Store model with minimal BIC over all  $\lambda_d, \lambda_W$  for risk-factor and  $M$ , subject to
        entropy constraints
    end
end

```

**Algorithm 1:** SCM learning and selection

Once subpopulations have been discovered with Algorithm 1, Algorithm 2 describes how survey-weighted GLMs estimate the association between each risk factor and each subpopulation. The strength of this association is captured by the risk factor's regression coefficient. We use both SCMs and GLMs because survey-weighted GLMs are required to obtain statistically valid parameter standard errors. For HYP, the GLM is logistic regression. For SBP and DBP, the GLM is linear regression. Separate GLMs are learned for the two types of continuous blood pressure because the multivariate regression problem becomes decomposable. Given a learned GLM, we care about three quantities: the  $p$ -value, regression coefficient, and the regression coefficient's standard error associated with that GLM's environmental exposure variable. We restrict our attention to environmental exposure variables with positive regression coefficients.

Our method generates a very large number of GLMs, and each GLM performs a hypothesis test to assess the significance of that GLM's risk factor. Because so many hypothesis

tests are being performed, we perform Benjamini-Hochberg false discovery rate (FDR) correction (Benjamini and Hochberg (1995)) on the  $p$ -values before assessing significance at a threshold of 0.02. All  $p$ -values reported in the next sections are post-adjustment.

```

Input: Response-variable, control-variables, set of risk factor categories, number of
       cadres  $M$ , set of optimal cadre models from Algorithm 1
Output: Set of survey-weighted generalized linear models for each cadre
for every category of risk factors in categories do
  for every risk-factor in category do
    for  $m = 1, \dots, M$  do
      Select all subjects  $X_m$  belonging to cadre  $m$  from risk factor's optimal SCM
      Learn and store survey-weighted GLM on  $X_m$  using risk-factor and all
      control-variables
    end
  end
end

```

**Algorithm 2:** Subpopulation-based survey-weighted generalized linear modeling

## 4.2 Summary of Results

First we summarize the study's results. In Section 4.3, we will examine specific subpopulations. Of the 218 risk factors we considered, 25 had a significant association with at least one response variable at an  $\alpha = 0.02$  significance threshold. Eleven significant associations and eight unique risk factors would not have been identified had we only modeled risk on a population-level. We take the log-odds ratios corresponding to significant risk factors and plot them in Fig. 1.

Some risk factors, such as the blood cadmium, are significant for more than one of our three response variables. Blood lead (LBXBPP) and blood cadmium (LBXBPD) are significant for all three response variables. In addition, 2-phenanthrene (URXP07) is significant for HYP and DBP, and nicosulfuron (URXNOS), mono-n-octyl phthalate (URXMOP), and urinary beryllium (URXUBE) are significant for DBP and SBP. Some of these associations have been discovered in previous studies. For example, Gallagher and Meliker (2010) found a positive association between blood cadmium and systolic and diastolic blood pressure for women, Nash et al. (2003) found a positive association between blood lead and SBP, DBP, and HYP in women, and Ranjbar et al. (2015) found a positive association between high blood pressure and 2-phenanthrene (URXP07). Thus, the SCM is capable of recovering the findings of multiple previous studies in a single analysis; it can also suggest new possible risk factors.

## 4.3 Discovered Subpopulations

In this section, we explore the subpopulations that the SCM discovers for selected risk factors. We summarize all cadre-assignment weights for SCMs that yield significant associations in Fig. 2. Age and gender are frequently important for determining cadre membership. From the hierarchical clustering with respect to covariates, we see that the assignment weights for ethnicities other than Non-Hispanic White are similar to each other, but dissimilar to the assignment weights for Non-Hispanic White. Thus, a given cadre structure

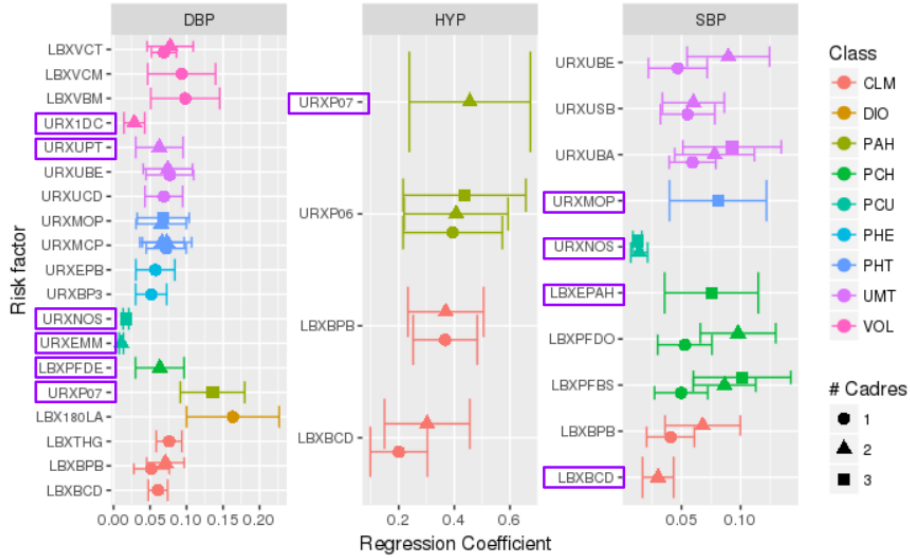


Figure 1: Distribution of regression coefficients corresponding to risk factors that are significant at the (adjusted)  $\alpha = 0.02$  level, shown with 95% confidence intervals. Boxed variables indicate significant associations that are only found because subpopulation-level modeling was utilized.

is likely to depend on either `Eth_White` and no other ethnicities, or it will depend on the ethnicities other than white.

Now we examine individual cadre structure in detail. Because of space constraints, we focus on only a few of the significant risk factors. The results for the other risk factors are available online, along with the scripts we used for modeling<sup>1</sup>. As we discuss regression coefficients and distributional means, recall that all continuous variables, including SBP and DBP, have been standardized and mean-centered. Throughout,  $M$  is refers to the number of cadres in the model: saying that a risk factor is significant at the  $M = 2$  level means that, after an SCM using that risk factor with  $M = 2$  was trained, at least one of the GLMs for a discovered subpopulations had a significant association between the response and the risk factor.

#### 4.3.1 BLOOD CADMIUM

In this section, we explore the subpopulations the SCM discovers when blood cadmium is included as a risk factor. Blood cadmium (LBXBCD, category CLM1) is a significant risk factor on the population-level (i.e., with  $M = 1$ ) for DBP (regression coefficient =  $0.061 \pm 0.007$ ,  $p < 10^{-10}$ ). It is a significant risk factor for HYP and SBP at an  $M = 1$  and  $M = 2$  level. For HYP and SBP, cadre modeling extracts subpopulations with stronger associations between LBXBCD and the response than the general population has.

1. URL will be included in final version.

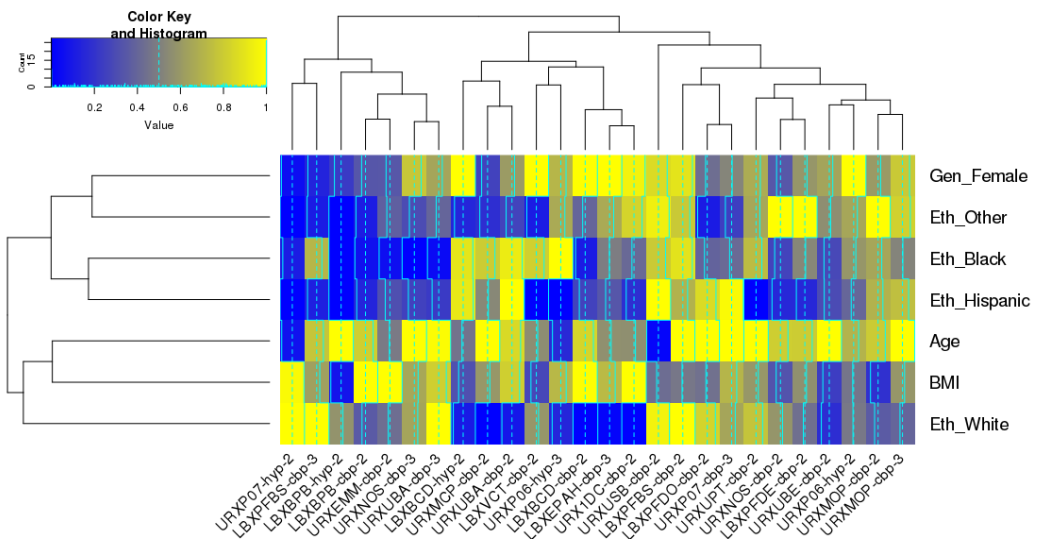


Figure 2: Cadre-assignment weights  $d$  for each SCM that yielded a significant GLM. The rownames indicate what model the weight vector  $d$  corresponds to: e.g., URXP07-hyp-2 (leftmost column) is the weight vector for the HYP  $M = 2$  SCM that included URXP07 as a covariate. Rows and columns are sorted by similarity, and each vector  $d$  has been standardized to have a maximum value of 1. Solid blue lines help map hues to numeric values in the key, and dotted blue lines show a reference value of 0.5.

First we consider the HYP model. At a population level, LBXBCD had a significant association with HYP ( $\log \text{odds ratio} = 0.20 \pm 0.05, p < 10^{-3}$ ). Now we examine the  $M = 2$  model's subpopulations. In the first (Cadre 1), there was no significant association between LBXBCD and HYP. In the second (Cadre 2), there was a significant association ( $\log \text{odds ratio} = 0.30 \pm 0.08, p < 10^{-3}$ ). Note that this subpopulation has a larger log-odds ratio than the population does as a whole. Thus, the SCM has pulled out the subjects who have an especially strong association between HYP and LBXBCD.

Investigation reveals that Cadre 2 was composed exclusively of women. This is similar to the findings of Gallagher and Meliker (2010), where blood cadmium had a significant positive association with SBP and DBP for women. Note that Gallagher and Meliker (2010) chose to analyze women separately, whereas we recovered this informative subpopulation automatically. There was a significant difference in mean LBXBCD between the two cadres as well (difference = 0.1690448,  $p < 10^{-10}$ ). This suggests follow-up questions: Why do women tend to have a higher concentration of blood cadmium, and why is a higher concentration of blood cadmium associated with risk for hypertension in women specifically?

Now we consider the SBP models. There was a population-level significant association between LBXBCD and SBP (regression coefficient =  $0.021 \pm 0.007, p < 10^{-2}$ ). When considering two subpopulations, in the first (Cadre 1), there was a significant association between LBXBCD and SBP (regression coefficient =  $0.030 \pm 0.007, p < 10^{-4}$ ). In the second (Cadre 2), there was no significant association. As with the HYP models, the subpopulation-level regression coefficient was larger than the population-level regression coefficient.

We visualize the subpopulation structure in Fig. 3. In Fig. 3a, we see that the subpopulation with a significant association between SBP and LBXBCD (Cadre 1) is composed primarily of subjects under the age of 40; for subjects near the age of 40, having a lower BMI makes you more likely to belong to Cadre 1. In Figs. 3b and 3c, we see that subjects in the subpopulation with a significant association between SBP and LBXBCD tend to have lower SBP and blood cadmium values than subjects in the other subpopulation do. The interesting question is why do these subjects, who have generally have a healthier SBP, have a significant association between SBP and blood cadmium?

#### 4.3.2 NICOSULFURON

In this section, we explore the subpopulations the SCM discovers when nicosulfuron is included as a risk factor. Nicosulfuron (URXNOS, category PCU2) is a significant risk factor for DBP in the  $M = 3$  SCM, and it is a significant risk factor for SBP in the  $M = 2$  and  $M = 3$  SCMs. That is, population-level modeling does not pick up nicosulfuron as a significant risk factor. We focus on the case where  $M = 3$  because then we can discuss a single set of subpopulations.

Nicosulfuron is significantly associated with DBP in a single subpopulation, Cadre 2 (regression coefficient =  $0.017 \pm 0.002, p < 10^{-4}$ ); it is also significantly associated with SBP in a single subpopulation, Cadre 1, (regression coefficient =  $0.012 \pm 0.002, p < 10^{-6}$ ). We visualize aspects of this subpopulation in Fig. 4. In Fig. 4a, we see that Cadre 1, for which there is a significant association between URXNOS and SBP, is composed almost entirely of white people older than their mid-thirties. Cadre 2, for which there is a significant

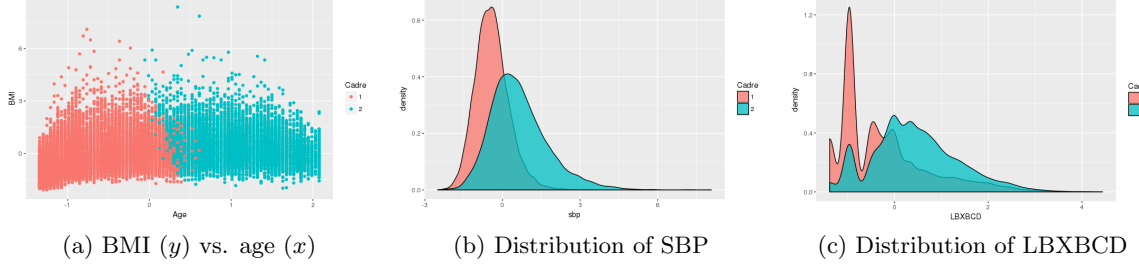


Figure 3: Visualizations of the CBP-response LBXBCD subpopulations, colored by subpopulation. In cadre 1 (red), there is a significant association between SBP and LBXBCD; in cadre 2 (blue), there is not. Cadre 1 is composed primarily of people under the age of 40, and its members have generally lower SBP and LBXBCD values than the members of Cadre 2 do.

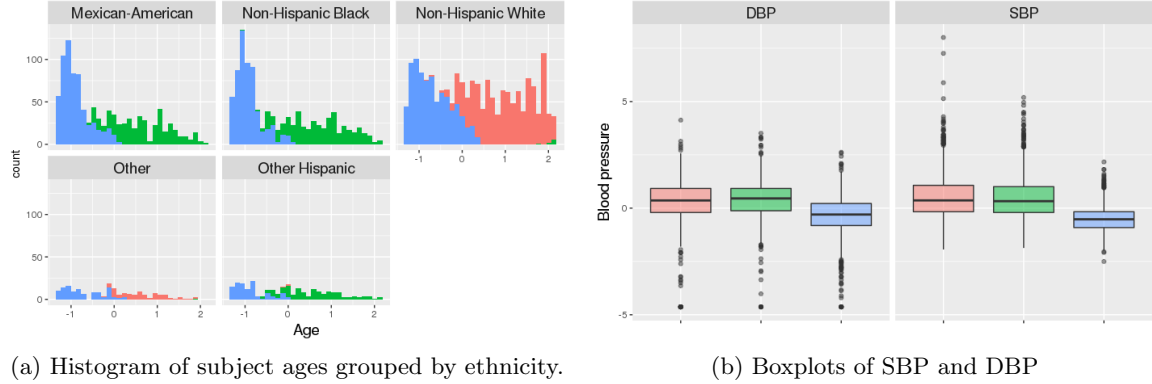


Figure 4: Visualizations of the CBP-response URXNOS subpopulations, colored by subpopulation. Cadres 1 (red, middle-aged and older white people) and 2 (green, middle-aged and older non-white people) have URXNOS as a significant risk factor. They also have higher blood pressures.

association between URXNOS and DBP, is composed of non-white people older than their mid-thirties. In Fig. 4b, we see that the subjects in Cadres 1 and 2 have higher SBP and DBP than the subjects in Cadre 3, for which URXNOS is not a significant risk factor. Further research could investigate why these specific subpopulations have these significant associations.

## 5. Discussion

In this paper, the supervised cadre model was used for a large-scale environmental association study that looked for risk factors associated with systolic and diastolic blood pressure and hypertension. Our EWAS workflow is a generalization of the standard EWAS, which is performed only on a population-level. In our EWAS, we analyzed more than two hundred

risk factors. Twenty-five risk factors had a significant association with at least one response variable; of these, eleven significant associations and eight unique risk factors were discovered due to our use of cadre modeling. Some of our significant associations agreed with other environmental risk factor analyses, while others are novel findings. The SCM learns interpretable subpopulations based on only a small number of covariates, and analysis of these subpopulations suggests further research questions.

Association studies have a major shortcoming: they are unable to deduce whether an identified association is causal or merely correlative (Patel et al. (2010)). Thus, we cannot be confident that any of the associations we discovered are causal in nature. However, our use of FDR correction and a low significance threshold means that our significant associations are unlikely to be spurious. Thus, our findings could motivate a longitudinal study.

Our methods are applicable to types of analysis other than the EWAS: we have demonstrated how the SCM can be applied to general risk analysis problems. We extended the SCM formalism from New et al. (2018) in three ways: (1) the SCM now supports multivariate regression and classification problems, (2) the SCM can be applied to data generated by a complex survey design, and (3) the uncertainty in the cadre assignment process can be quantified via the estimation of a conditional entropy. Future work could apply this framework to genomics-based precision health problems, such as variant of uncertainty analysis for breast cancer (Easton et al. (2007)).

## References

M. Abadi et al. TensorFlow: Large-scale machine learning on heterogeneous systems, 2015. URL <https://www.tensorflow.org/>. Software available from tensorflow.org.

Y. Benjamini and Y. Hochberg. Controlling the false discovery rate: A practical and powerful approach to multiple testing. *Journal of the Royal Statistical Society Series B (Methodological)*, 57(1):289–300, 1995.

Centers for Disease Control and Prevention (CDC). National Health and Nutrition Examination Survey. URL <http://www.cdc.gov/nchs/nhanes/>.

C. Colijn, N. Jones, I. G. Johnston, S. Yaliraki, and M. Barahona. Toward precision healthcare: Context and mathematical challenges. *Frontiers in Physiology*, 8:136, 2017. ISSN 1664-042X. doi: 10.3389/fphys.2017.00136. URL <https://www.frontiersin.org/article/10.3389/fphys.2017.00136>.

A. Demiriz, K. P. Bennett, and M. J. Embrechts. Semi-supervised clustering using genetic algorithms. In *In Artificial Neural Networks in Engineering (ANNIE-99)*, pages 809–814. ASME Press, 1999.

F. Doshi-Velez and B. Kim. Towards A Rigorous Science of Interpretable Machine Learning. *arXiv e-prints*, February 2017.

D. F. Easton, A. M. Deffenbaugh, D. Pruss, C. Frye, R. J. Wenstrup, K. Allen-Brady, S. V. Tavtigian, A. N. Monteiro, E. S. Iversen, F. J. Couch, and D. E. Goldgar. A systematic genetic assessment of 1,433 sequence variants of unknown clinical significance

in the BRCA1 and BRCA2 breast cancer-predisposition genes. *Am. J. Hum. Genet.*, 81(5):873–883, Nov 2007.

C. M. Gallagher and J. R. Meliker. Blood and urine cadmium, blood pressure, and hypertension: a systematic review and meta-analysis. *Environ. Health Perspect.*, 118(12):1676–1684, Dec 2010.

W. G. Gathirua-Mwangi, T. W. Zollinger, M. J. Murage, K. R. Pradhan, and V. L. Champion. Adult BMI change and risk of Breast Cancer: National Health and Nutrition Examination Survey (NHANES) 2005-2010. *Breast Cancer*, 22(6):648–656, Nov 2015.

A. Gelman, J.B. Carlin, H.S. Stern, D.B. Dunson, A. Vehtari, and D.B. Rubin. *Bayesian Data Analysis, Third Edition*. Chapman & Hall/CRC Texts in Statistical Science. Taylor & Francis, 2013. ISBN 9781439840955.

S. Heeringa, B. West, and P. Berglund. *Applied Survey Data Analysis*. Chapman and Hall/CRC., 2 edition, 2017.

M. I. Jordan and R. A. Jacobs. Hierarchical mixtures of experts and the EM algorithm. *Neural Comput.*, 6(2):181–214, March 1994. ISSN 0899-7667. doi: 10.1162/neco.1994.6.2.181. URL <http://dx.doi.org/10.1162/neco.1994.6.2.181>.

D. P. Kingma and J. Ba. Adam: A method for stochastic optimization. *CoRR*, abs/1412.6980, 2014. URL <http://arxiv.org/abs/1412.6980>.

Z. C. Lipton. The mythos of model interpretability. *CoRR*, abs/1606.03490, 2016. URL <http://arxiv.org/abs/1606.03490>.

T. Lumley. survey: analysis of complex survey samples, 2016. R package version 3.32.

K. P. Murphy. *Machine Learning: A Probabilistic Perspective*. The MIT Press, 2012. ISBN 9780262018029.

D. Nash, L. Magder, M. Lustberg, et al. Blood lead, blood pressure, and hypertension in perimenopausal and postmenopausal women. *JAMA*, 289(12):1523–1532, 2003. doi: 10.1001/jama.289.12.1523. URL <http://dx.doi.org/10.1001/jama.289.12.1523>.

A. New, C. Breneman, and K. P. Bennett. Cadre modeling: Simultaneously discovering subpopulations and predictive models. In *2018 International Joint Conference on Neural Networks (IJCNN)*, 2018. URL <https://arxiv.org/abs/1802.02500>. To appear.

C. J. Patel, J. Bhattacharya, and A. J. Butte. An environment-wide association study (EWAS) on type 2 diabetes mellitus. *PLOS ONE*, 5(5):1–10, 05 2010. doi: 10.1371/journal.pone.0010746. URL <https://doi.org/10.1371/journal.pone.0010746>.

M. Ranjbar, M. A. Rotondi, C. I. Ardern, and J. L. Kuk. Urinary Biomarkers of Polycyclic Aromatic Hydrocarbons Are Associated with Cardiometabolic Health Risk. *PLoS ONE*, 10(9):e0137536, 2015.

- I. Shiue. Higher urinary heavy metal, phthalate, and arsenic but not parabens concentrations in people with high blood pressure, U.S. NHANES, 2011-2012. *Int J Environ Res Public Health*, 11(6):5989–5999, Jun 2014.
- R. Tibshirani. Regression shrinkage and selection via the lasso. *Journal of the Royal Statistical Society, Series B*, 58:267–288, 1994.
- L. Trasande, S. Sathyannarayana, A. J. Spanier, H. Trachtman, T. M. Attina, and E. M. Urbina. Urinary phthalates are associated with higher blood pressure in childhood. *The Journal of Pediatrics*, 163(3):747 – 753.e1, 2013. ISSN 0022-3476.
- X. Wang, Y. Wang, and L. Wang. Improving fuzzy c-means clustering based on feature-weight learning. *Pattern Recognition Letters*, 25(10):1123 – 1132, 2004. ISSN 0167-8655. doi: <https://doi.org/10.1016/j.patrec.2004.03.008>.
- D. M. Witten and R. Tibshirani. A framework for feature selection in clustering. *Journal of the American Statistical Association*, 105(490):713–726, 6 2010. ISSN 0162-1459. doi: 10.1198/jasa.2010.tm09415.
- H. Zou and T. Hastie. Regularization and variable selection via the elastic net. *Journal of the Royal Statistical Society, Series B*, 67:301–320, 2005.